

## ORIGINAL ARTICLE

# Buckwheat UDP-Glycosyltransferase *FtUGT71K6* and *FtUGT71K7* Tandem Repeats Contribute to Drought Tolerance by Regulating Epicatechin Synthesis

Yuanfen Gao<sup>1,2,3</sup> | Yaliang Shi<sup>2,3</sup> | Tanzim Jahan<sup>2,3</sup> | Md. Nurul Huda<sup>2,3</sup>  | Lin Hao<sup>2,3</sup> | Yuqi He<sup>2,3</sup> | Muriel Quinet<sup>4</sup> | Hui Chen<sup>1</sup>  | Kaixuan Zhang<sup>2,3</sup> | Meiliang Zhou<sup>2,3</sup> 

<sup>1</sup>College of Life Sciences, Sichuan Agricultural University, Ya'an, Sichuan, China | <sup>2</sup>National Key Facility for Crop Gene Resources and Genetic Improvement/Key laboratory Grain Crop Genetic Resources Evaluation and Utilization Ministry of Agriculture and Rural Affairs, Beijing, Haidian District, China | <sup>3</sup>Institute of Crop Sciences, Chinese Academy of Agricultural Sciences, Beijing, Haidian District, China | <sup>4</sup>Groupe de Recherche en Physiologie Végétale (GRPV), Earth and Life Institute-Agronomy (ELI-A), Université Catholique de Louvain, Louvain-la-Neuve, Belgium

**Correspondence:** Hui Chen ([chenhui@sicau.edu.cn](mailto:chenhui@sicau.edu.cn)) | Kaixuan Zhang ([zhangkaixuan@caas.cn](mailto:zhangkaixuan@caas.cn)) | Meiliang Zhou ([zhoumeiliang@caas.cn](mailto:zhoumeiliang@caas.cn))

**Received:** 30 July 2024 | **Revised:** 11 November 2024 | **Accepted:** 8 January 2025

**Funding:** This research was supported by National Key Research and Development Program of China (2022YFE0140800), National Natural Science Foundation of China (32161143005).

**Keywords:** buckwheat | drought stress | epicatechin | *FtUGT71K6* | *FtUGT71K7* | UDP-glycosyltransferase

## ABSTRACT

Glycosyltransferase genes are organised as tandem repeats in the buckwheat genome, yet the functional implications and evolutionary significance of duplicated genes remain largely unexplored. In this study, gene family analysis revealed that *FtUGT71K6* and *FtUGT71K7* are tandem repeats in the buckwheat genome. Moreover, GWAS results for epicatechin suggested that this tandem repeat function was associated with epicatechin content of Tartary buckwheat germplasm, highlighting variations in the promoter haplotypes of *FtUGT71K7* influenced epicatechin levels. *FtUGT71K6* and *FtUGT71K7* were shown to catalyse UDP-glucose conjugation to cyanidin and epicatechin. Furthermore, overexpression of *FtUGT71K6* and *FtUGT71K7* increased total antioxidant capacity and altered metabolite content of the epicatechin biosynthesis pathway, contributing to improved drought tolerance, while overexpression of *FtUGT71K6* significantly improved salt stress tolerance. However, overexpression of these two genes did not contribute to resistance against *Rhizoctonia solani*. Evolutionary selection pressure analysis suggested positive selection of a critical amino acid ASP-53 in *FtUGT71K6* and *FtUGT71K7* during the duplication event. Overall, our study indicated that *FtUGT71K6* and *FtUGT71K7* play crucial roles in drought stress tolerance via modulating epicatechin synthesis in buckwheat.

## 1 | Introduction

Glycosyltransferases are the executors of the glycosylation of secondary metabolites in plants, including flavonoids (Lim et al. 2004), terpenoids (Caputi et al. 2012), and hormones (Dong et al. 2014). Glycosylation alters the physical properties of these compounds, such as hydrophilicity and stability

(Vogt and Jones 2000; Bowles et al. 2005), and influences their biological activities, including antioxidant capacity (Zheng et al. 2017), cellular accumulation (Jones and Vogt 2001), stress tolerance (Zhao et al. 2019), inter-tissue transport (Bönisch et al. 2014), and subcellular localisation (Bowles et al. 2006). Many glycosyltransferases exhibit multisubstrate catalytic functions, enabling them to influence the synthesis and activity

The first two authors contributed equally to this work.

of multiple compounds simultaneously (Griesser et al. 2008). Gene family analyses have revealed that numerous UGTs are present in plant genomes, often occurring as tandem duplications, that is, apple (Velasco et al. 2010), wheat (He et al. 2018), cotton (Xiao et al. 2019), pomelo (Wu et al. 2020), and buckwheat (Yang et al. 2024). Despite their abundance, relatively few UGTs have been functionally characterised in plants (Gachon, Langlois-Meurinne, and Saindrenan 2005). For instance, the function of the UGT71 subfamily is yet unexplored, which is the largest subfamily of buckwheat UGTs (Yang et al. 2024).

Flavan-3-ols, a class of flavonoids, including compounds such as catechins and epicatechins (Huda et al. 2021). They are biosynthesized through the action of leucocyanidin reductase (LAR) and anthocyanidin reductase (ANR), which facilitate the formation of anthocyanins and eventually polymerise to form proanthocyanidins (Tanner et al. 2003). These compounds possess antioxidant properties, largely influenced by the number of their phenolic hydroxyl group (Cos et al. 2004). The phenolic hydroxyl groups donate electrons that stabilise free radicals, while the aromatic ring is stabilised by aryl resonance, allowing effective radical scavenging activity (Riceevans et al. 1995; Cao, Sofic, and Prior 1997; Fujisawa and Kadoma 2006). The antioxidant activity of flavan-3-ols contributes to plant tolerance against various environmental stresses (Mierziak, Kostyn, and Kulma 2014; Nakabayashi et al. 2014), such as salinity (Mahajan and Yadav 2014), drought (Nakabayashi et al. 2014), water deficit (Yuan et al. 2012), and cold (Meng et al. 2015). Both anthocyanins and flavan-3-ols undergo glycosylation, a modification that enhances their solubility and facilitates the formation of proanthocyanidins (Marinova et al. 2007; Zhao and Dixon 2010; Slámová, Kapešová, and Valentová 2018).

Buckwheat is well known for its high flavonoid content, particularly rutin and epicatechin (Martín-García et al. 2019; Zamaratskaia et al. 2023). Various glycosyltransferases have been identified in buckwheat that are functionally distinct and play crucial roles in flavonoid biosynthesis (Zhou et al. 2016; Yin et al. 2020; Zhang, He, et al. 2021). However, the function of epicatechin-related glycosyltransferases in Tartary buckwheat remain underexplored. Metabolite genome-wide association study (mGWAS) provides an efficient approach for mining metabolite-related genes (Zhang, He, et al. 2021; Zhao, He, et al. 2023). Based on the mGWAS findings, we identified multiple tandem glycosyltransferases in a highly linkage region of the epicatechin GWAS leading SNP. Haplotype analysis, enzyme function validation, flavonoid content assay, and resistance phenotype analysis of overexpressed buckwheat hairy roots and *Arabidopsis thaliana* were performed to elucidate *FtUGT71K7*'s role in epicatechin synthesis. We also found that *FtUGT71K6* exhibits similar functional characteristics. Overall, this study highlights the pivotal role of tandem glycosyltransferases *FtUGT71K6* and *FtUGT71K7* in epicatechin biosynthesis of buckwheat in response to abiotic stresses. Therefore, our findings provide new insights into the biosynthesis of epicatechin in buckwheat.

## 2 | Methods

### 2.1 | Identification of UGT71 Subfamily Genes and Their Chromosomal Position in the Buckwheat Genome

The genome data for *Fagopyrum tataricum*, *Fagopyrum esculentum* var. *homotropicum*, *Fagopyrum esculentum*, and *Fagopyrum dibotrys* were downloaded from the Buckwheat Genome Project Database (GPDB) (<http://47.93.16.146/home#/home>) (Zhang, He, et al. 2021; He et al. 2022; He et al. 2023a; Zhang et al. 2023). Another study found UGT family genes in *F. tataricum* and *F. esculentum* var. *homotropicum* (Zhang et al. 2023). UGT71 genes in *F. dibotrys*, *F. esculentum*, *F. tataricum*, and *F. esculentum* var. *homotropicum* were identified by BLAST v2.9.0 with a sequence identity threshold of over 75%. The Conservative Domain Search Service (Batch CD-Search) and SMART tools were employed to verify conserved domains. Motif analysis in UGT71 was performed using MEME (<http://meme.nbcr.net/meme/intro.html>). Sequence length, molecular weight, and isoelectric point (*pI*) of UGT71 proteins were calculated using tools available on the ExPASy website ([https://web.expasy.org/compute\\_pi/](https://web.expasy.org/compute_pi/)).

For phylogenetic analysis, full-length amino acid sequences of UGT71 proteins from *Arabidopsis thaliana*, *Pyrus communis*, *Pyrus x bretschneideri*, *Malus sylvestris*, *Malus domestica*, *Prunus avium*, *Prunus mume*, *Prunus persica*, *Prunus dulcis*, *Prunus yedoensis* var. *nudiflora*, and *Prunus persica* were used. After full-length amino acid sequences of all UGT71 were aligned using MUSCLE v3.8, a phylogenetic tree was constructed with the maximum likelihood method by IQ-TREE 1.6.12 software with the parameter '-m JTT+G4 -b 1000' (Sleator 2016). The chromosomal distribution of UGT71 genes across the four buckwheat genomes was retrieved and visualised using TBtools. Potential gene duplication events among *FtUGT71s*, *FhUGT71s*, *FeUGT71s*, and *FdUGT71s* were investigated using the Python Multiple Collinear Scanning toolkit (JCVI) (Tanenbaum et al. 2010; Sleator 2016).

### 2.2 | Genome-Wide Association Study (GWAS)

The genotyping datasets of 200 mini-core accessions of buckwheat were obtained from a previous study (Zhao, He, et al. 2023). SNPs were filtered based on a minor allele frequency (MAF  $\geq 0.05$ ) and a missing rate of  $\leq 0.1$  using VCFtools for subsequent analysis. Whole-genome association analysis on flavonoid metabolite content in Tartary buckwheat was conducted using the factorial spectral transform linear mixed model (FaST-LMM) (Lippert et al. 2011). Based on the effective number of tests, the threshold ( $P = 1/N_e$ ) was set at  $1 \times 10^{-5}$ . The Manhattan and Q-Q plots were visualised by the R software with the CMplot package. Candidate genes were identified within a 100-kb flanking region of significant loci, determined by the whole-genome linkage disequilibrium (LD) decay distance. The haplotypes of the candidate genes were analyzed using Candihap software (Li et al. 2023).

## 2.3 | Establishment of *FtUGT71K6* and *FtUGT71K7* Overexpressing Hairy Roots and *Arabidopsis*

The method for establishing overexpressed hairy root lines was adapted from Gabr et al. (2019). Total RNA from Tartary Buckwheat cv. Pinku leaves were extracted using the FastPure Universal Plant Total RNA Isolation Kit (Vazyme, China), and cDNA was synthesised with the HiScript II 1st Strand cDNA Synthesis Kit (Vazyme, China). PCR amplification of *FtUGT71K6* and *FtUGT71K7* was performed by 2×Phanta Max Master Mix, using primers listed in Supporting Information S2: Table S5. The *FtUGT71K6* and *FtUGT71K7* genes were individually cloned into the *pCAMBIA1307-myc* vector (*35S:FtUGT71K6-cmyc*, *35S:FtUGT71K7-cmyc*). *Agrobacterium rhizogenes* strain A4, suspended in Murashige & Skoog (MS) liquid medium, was used to infect Tartary buckwheat cv. Pinku explants for 12 min. The explants were then incubated in the dark on MS solid medium for 2 days before being transferred to MS solid plates containing Hygromycin B. Positive lines were confirmed by extracting DNA from the hairy roots using the CTAB method (Irsyadi et al. 2024). On the other hand, the floral dip method was used for *A. thaliana* (Col-0) transformation (Chen and Murata 2002). The constructed vectors were introduced into *Agrobacterium tumefaciens* strain GV3101, and positive clones were selected and cultured in the YEB liquid medium until reaching an optical density (OD) of 0.6. The *Agrobacterium* suspension was prepared in a 5% sucrose solution containing 0.05% acetosyringone, and 4-week-old *Arabidopsis* (Col-0) seedlings were transformed using the floral dip method to obtain overexpression lines.

## 3 | UHPLC/MS

Flavonoids, anthocyanins, and proanthocyanidins in the overexpressed hairy root and *Arabidopsis* samples were quantified using the 6475 Triple Quadrupole LC/MS System (Agilent, US). Plant samples were freeze-dried at  $-80^{\circ}\text{C}$ , and the overexpression of hairy roots was processed according to the method described by Zhang et al. (2018). Freeze-dried plant material was ground to a powder, dissolved in 80% (v/v) aqueous methanol, and sonicated for 45 min. The supernatant was then filtered into vials for analysis. UHPLC was performed using a 6490 Triple Quadrupole LC/MS System equipped with an ESI-triple quadrupole-linear ion trap (QTRAP)-MS. The UHPLC conditions were: Waters X Select HSS T3 (2.1 mm × 100 mm × 1.8 μm); 0.1% formic acid purified with water (A) and acetonitrile (B). The gradient program was as follows: the starting conditions of 98% A, 2% B, to 4 min, turning to 5% A within 11 min, a linear gradient of 20% B, until 13 min, 2% B, and a composition of 98% B were kept for 2 min. Three biological replicates were measured for each sample.

### 3.1 | Recombinant Protein Purification and Enzyme Assay

For protein extraction, overexpressed hairy roots of *FtUGT71K6* and *FtUGT71K7* were utilised. Freshly weighed overexpressed

hairy roots (5 g) were ground in liquid nitrogen and added to Tris-HCl buffer (containing 100 mM Tris-HCl, 250 mM NaCl, 1 mM DTT, 0.05% β-mercaptoethanol, 1 mM PMSF, and Roche cOmplete Protease Inhibitor Cocktail (EDTA-free) at pH 7.0). The mixture was incubated at  $4^{\circ}\text{C}$  for 10 min. BeyoMag™ Anti-Myc Magnetic Beads (Beyotime, China) were used for protein purification, with the beads washed three times with the Tris-HCl buffer. The protein was eluted by a buffer containing c-myc peptide (Beyotime, China). For the *FtUGT71K6* and *FtUGT71K7* activity assays, the reaction buffer comprised 100 mM Tris-HCl (pH 7.0), 0.5 mM cyanidin/epicatechin (CAS: 528-58-5, 490-46-0, Shanghai, China), 5 mM UDP-glucoside, and 0.1 mM  $\text{MgCl}_2$ . To this, 0.5 μg of purified protein was added and incubated at  $30^{\circ}\text{C}$  for 30 min. The reaction products were freeze-dried at  $-40^{\circ}\text{C}$ , redissolved in 80% methanol, and analyzed by UHPLC-MS using the 6530 LC/Q-TOF system (Agilent).

### 3.2 | Subcellular Localisation

*FtUGT71K6* and *FtUGT71K7* genes were cloned into the *pCAMBIA1305-GFP* vector using primers listed in Supporting Information S2: Table S5. The recombinant vectors were transformed into *Agrobacterium tumefaciens* strain GV3101. The bacterial cells were resuspended in MES buffer (10 mM MES, 10 mM  $\text{MgCl}_2$ , and 1 mM acetosyringone) and incubated in the dark for 2 h. Following incubation, the suspension was injected into 4-week-old tobacco plants, which were subsequently incubated for 24 h in the dark, followed by 24 h in light. Subcellular localisation was visualised using a Laser Scanning Confocal Microscope (Zeiss LSM900).

### 3.3 | Total RNA Extraction, cDNA Synthesis, and qRT-PCR Analysis

Transcript levels of overexpressed hairy roots were quantified using fluorescence-based relative quantification (Livak and Schmittgen 2001). Total RNA was extracted from plant samples using RNA Easy Fast Extraction Kits (TIANGEN, China). Afterward, reverse transcription was carried out using the PrimeScript First-Strand cDNA Synthesis Kit (Takara). For transcriptional analysis, a SYBR Green-based assay (SYBR Master Mix Ex Taq, Takara) was used with cDNA and primer mix on a BIO-RAD CFX96 real-time PCR system (Bio-Rad Laboratories, Hercules, CA, USA). Primer sequences are provided in Supporting Information S2: Table S5. Relative expression of the overexpressed lines was calculated using the  $2^{-\Delta\Delta C_t}$  method (Livak and Schmittgen 2001).

### 3.4 | Luciferase Reporter

The *pGreenII-0800-LUC* system was utilised to assess the activity of the *FtUGT71K7* promoter in different haplotypes. Genomic DNA from Tartary buckwheat material GS163 (Hap 1) and SX-37 (Hap 3) served as templates to clone the promoter of *FtUGT71K7*. The  $-2000$  bp to  $-1700$  bp promoter regions of *FtUGT71K7* from Hap1 and Hap3 were cloned and transformed

into *Agrobacterium rhizogenes* strain GV3101 (ZOMANBIO, Beijing, China). Primers are listed in Supporting Information S2: Table S5. Positive clones were selected using rifampicin and kanamycin, then cultured until reaching an optical density (OD) of 0.8 and resuspended in 0.2 mM MES buffer (containing 1 mM MgCl<sub>2</sub> and 0.1 mM acetosyringone). After that, the resuscitation fluid was injected into tobacco leaves. The Bio-Glo-NL Luciferase Assay System (Promega, US) was used to detect LUC activity.

### 3.5 | Abiotic and Biotic Stress Treatments

For drought and salt stress, 10% PEG and 80 mM NaCl were applied, respectively. Overexpressed *Arabidopsis* seeds were germinated on MS solid medium, and uniformly germinated *A. thaliana* seedlings and hairy roots were then transferred to MS solid medium containing either 10% PEG or 80 mM NaCl. Fresh weight of hairy roots was weighed after removing the MS solid medium. Root length of *A. thaliana* was recorded after 7 days, and the weight of hairy roots was assessed after 14 days. Soil-grown *A. thaliana* plants were manually watered five times over 20 days, followed by a cessation of watering to measure the weight of the upper leaves after an additional 21 days. For biotic stress, isolated leaves of *A. thaliana* seedlings were inoculated with *Rhizoctonia solani* AG4-HGI 3 (Li et al. 2021) and incubated in the dark at 28°C for 24 h (He et al. 2023b).

### 3.6 | Determination of Superoxide, Antioxidant Enzyme Activities, Proline, Soluble Sugar, MDA Content, and Total Antioxidant Capacity

Rosette leaves of *Arabidopsis* plants were grown under uniform growth conditions and used as samples for staining. Hydrogen peroxide (H<sub>2</sub>O<sub>2</sub>) and superoxide radicals were detected using diaminobenzidine (DAB) and nitroblue tetrazolium (NBT) staining, respectively (Du et al. 2008; Wang et al. 2011). Approximately 0.03 g of rosette leaves of *Arabidopsis* or hairy root samples were ground in liquid nitrogen, followed by the addition of extraction buffer provided in respective kits. The activities of superoxide dismutase (SOD), catalase (CAT), and peroxidase (POD) were measured using assay kits from Solarbio (Solarbio, Beijing, China). Malondialdehyde (MDA), proline (Pro), and soluble sugar content were also determined using Solarbio assay kits (Solarbio, Beijing, China). Total antioxidant capacity was measured by Total Antioxidant Capacity Assay Kit with ABTS method (Beyotime, Shanghai, China). Absorbance readings were obtained using a Synergy HTX Multi-Mode Microplate Reader (BioTek, USA). Each treatment was performed in three biological replicates.

### 3.7 | Analysis for Sites and Branches Under Selection Pressure

The selection pressure on sites and branches was analyzed using the Codeml program from PAML, which calculated the non-synonymous to synonymous substitution rate ratio (dN/dS or  $\omega$ ) based on codon-based nucleotide alignments (Erthmann,

Agerbirk, and Bak 2018). To investigate whether specific branches were subject to positive selection, the branch-site model (Model A) was employed, assuming that some sites on the foreground branch may be under positive selection ( $\omega > 1$ ), while sites on the background branches experience negative or neutral selection. A likelihood ratio test (LRT) was conducted to detect positive selection by comparing the log-likelihood values of Model A with the log-likelihood value of the corresponding null model, in which the  $\omega$  parameter is constrained to 1 (no positive selection). The statistical significance of the test was evaluated by calculating the difference in log-likelihood values ( $2\Delta\ln L$ ) and performing a  $\chi^2$  test ( $p < 0.05$ ).

### 3.8 | Statistical Analysis

ANOVA was used for statistical evaluations by Graphpad prism 8. The differences were considered significant at \* $p < 0.05$ , \*\* $p < 0.01$ , and \*\*\* $p < 0.001$ .

## 4 | Results

### 4.1 | Identification and Characterisation of UGT71 Subfamily Members in Buckwheat Genome

The *UGT71* subfamily, the largest in the Tartary Buckwheat genome, is predominantly organised as tandem repeats (Yang et al. 2024). To determine the conservation of the *UGT71* family across four buckwheat species, including *Fagopyrum tataricum*, *F. esculentum*, *F. dibotrys*, and *F. esculentum* var. *homotropicum*, a comprehensive gene family analysis was performed. Based on the UGT conserved structural domain, a total of 62 *UGT71* members were identified across these species, including 18 in Tartary buckwheat, 11 in *F. esculentum* var. *homotropicum*, 14 in golden buckwheat, and 19 in common buckwheat (Supporting Information S2: Table S1). All identified *UGT71* proteins were shorter than 600 amino acids (AA) (Supporting Information S2: Table S2), with their conserved domains mostly located near the C-terminus. Structural analysis revealed a generally low number of introns; the majority of *UGT71* genes have no introns, with only five genes containing two introns (Supporting Information S1: Figure S1). The lower number of introns is significant as it may facilitate faster transcription and rapid gene expression within the *UGT71* subfamily (Morgan, Fink, and Bartel 2019). Gene length distribution showed that most *UGT71* genes were under 2000 bp, with longer genes typically containing extended intronic regions. Notably, one *UGT71* gene in golden buckwheat, which exceeds 6000 bp, may have unique regulatory functions associated with its extended length (Supporting Information S1: Figure S1).

To classify and characterise these proteins, a phylogenetic tree was constructed using *UGT71* proteins from *Arabidopsis thaliana*, *Pyrus communis*, *Malus sylvestris*, and others. The analysis revealed that *UGT71* proteins across different species share similar motif distributions, with motif 3 consistently located at the C-terminal and motif 5 at or near the N-terminal (Figure 1a, Supporting Information S2: Table S2). This suggests similar

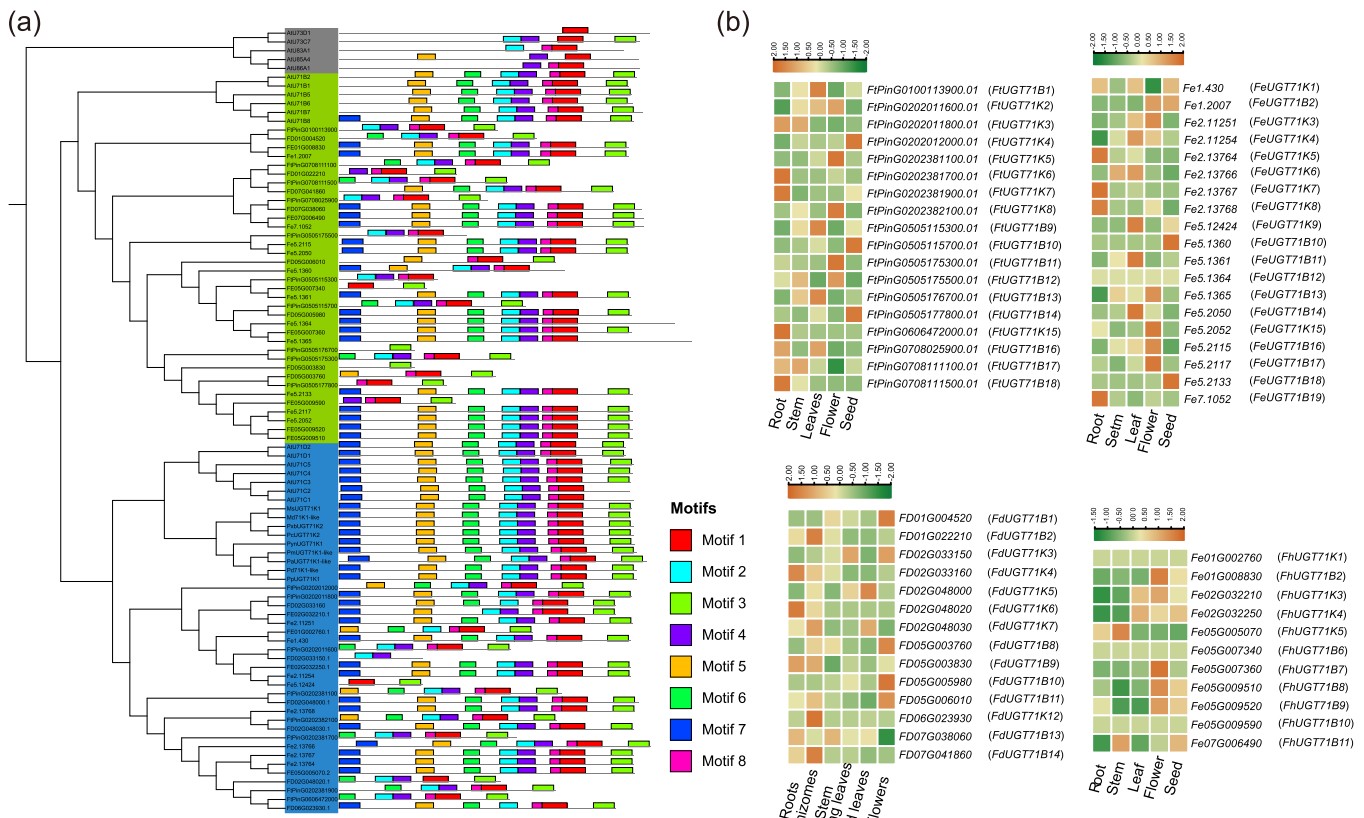


**FIGURE 1** | UGT71 subfamily identification and expression profiles in *F. esculentum*, *F. esculentum* var. *homotropicum*, *F. dibotrys*, and *F. tataricum*. (a) Unrooted phylogenetic tree indicating the relationship of UGT71 in the genera *Asterias tartaricus* and *Asterias dalianensis*. (b) Expression profiles of different tissues. [Color figure can be viewed at [wileyonlinelibrary.com](https://onlinelibrary.wiley.com)]

tertiary structures within the UGT71 subfamily. Buckwheat UGT71 subfamily proteins are more closely related to AtUGT71B and PcUGT71K, classifying them as UGT71B/K (Figure 1a, Supporting Information S2: Table S2). Expression pattern analysis showed varied expression modes among UGT71 genes (Figure 1b), with some closely related genes displaying similar expression patterns, such as *FtPinG0202381700.01*, *FtPinG0202381900.01*, *Fe2.13764*, *Fe2.13767*, and *Fe2.13767*, which are highly expressed in roots, while *Fe5.2115*, *Fe5.2117*, and *Fe5.2052* showed higher expression in flowers (Figure 1b). These consistent expression patterns among similar genes indicate potential functional similarities. Thus, our analysis of the UGT71 subfamily across four buckwheat species revealed conserved secondary structures and identified genes with similar expression patterns, providing insights into their potential functional roles.

#### 4.2 | UGT71 Subfamily Gene Duplication

Using genome databases of common buckwheat (*F. esculentum*), *F. esculentum* var. *homotropicum*, Tartary buckwheat (*F. tataricum*), and golden buckwheat (*F. dibotrys*), we generated physical maps to illustrate the genomic distribution of UGT71 subfamily members. The *FtUGT71* genes were distributed on chromosomes Ft1, Ft3, Ft5, Ft6, and Ft7; the *FdUGT71* genes on chromosomes Chr1, Chr2, Chr5, Chr6, and Chr7; the *FhUGT71* genes on chromosomes Chr1, Chr2, Chr5, and Chr7;

and the *FeUGT71* genes on chromosomes Chr1, Chr2, Chr5, and Chr7. Notably, multiple tandem duplication events were identified, with conserved chromosomal regions containing tandem duplications of *FtUGT71K3*, *FtUGT71K4*, *FtUGT71K5*, *FtUGT71K6*, *FtUGT71K7*, *FtUGT71K8* (*FtPinG0202011800*, *FtPinG0202012000*, *FtPinG0202381100.01*, *FtPinG0202381700.01*, *FtPinG0202381900.01* and *FtPinG0202382100.01*) on chromosome 2 and *FtUGT71B9*, *FtUGT71B10*, *FtUGT71B11* (*FtPinG0505115300*, *FtPinG0505115700.01*, and *FtPinG0505175300*) on chromosome 5 among buckwheat species (Supporting Information S1: Figure S2).

Covariance analysis was conducted on the four buckwheat species along with *Pleuropterus multiflorus* and *Rheum tanguticum* to explore the evolutionary relationships within the *FtUGT71* subfamily across buckwheat species and other members of the Polygonaceae family. The analysis revealed that homologous genes *UGT71K5*, *UGT71K6*, *UGT71K7*, *UGT71K8*, *UGT71B9*, *UGT71B10* and *UGT71B11* were located in amplification blocks at similar chromosomal positions across buckwheat species. However, this pattern was absent in *Pleuropterus multiflorus* and *Rheum tanguticum*, indicating that the UGT71 subfamily has been more conserved in buckwheat during interspecific evolution compared to other Polygonaceae species (Supporting Information S1: Figure S3). These findings indicate a high level of conservation for *UGT71K5*, *UGT71K6*, *UGT71K7*, *UGT71K8*, *UGT71B9*, *UGT71B10* and *UGT71B11* within buckwheat species.

### 4.3 | Association of *UGT71* Tandem Repeats With Epicatechin Biosynthesis in Tartary Buckwheat

Gene duplication has long been recognised as a driving force of evolutionary diversity, often leading to novel gene functions (Birchler and Yang 2022). To understand the role of *UGT71* tandem repeats, we analyzed available buckwheat GWAS data (Zhao, He, et al. 2023). Our analysis identified SNP Ft2:56627563 as significantly associated with epicatechin content (Figure 2a). Further analysis showed that this leading SNP and its locus are close to the tandem repeats *FtUGT71K5*, *FtUGT71K6*, *FtUGT71K7*, and *FtUGT71K8*, which were located within a 27-kb region near the leading SNP, suggesting a strongly linked region (Figure 2b). Additionally, SNPs Ft2:56616116 and Ft2:5661938 were significantly correlated with epicatechin-epiafzelechin and procyanidin A3 content, respectively (Supporting Information S1: Figure S4), suggesting an association between *FtUGT71K5*, *FtUGT71K6*, *FtUGT71K7*, and *FtUGT71K8* tandem repeats and epicatechin biosynthesis. Protein sequence similarity among *FtUGT71K5*, *FtUGT71K6*, *FtUGT71K7*, and *FtUGT71K8* was over 75% (Figure 2c), indicating potential functional redundancy.

To further investigate the association between *FtUGT71K5*, *FtUGT71K6*, *FtUGT71K7*, and *FtUGT71K8* tandem repeats and epicatechin content in buckwheat, we performed haplotype analysis of the candidate genes. Variants at positions -1906 bp (Hap1: C/C, Hap3: T/T) and -1895 bp (Hap1: T/T, Hap3: C/C) in the *FtUGT71K7* promoter classified 200 buckwheat samples into three haplotypes (Figure 2d, Supporting Information S2: Table S3). Haplotype analysis revealed that the Hap1 group had significantly higher epicatechin content compared to the Hap3 group (Figure 2e). Correspondingly, the transcription level of *FtUGT71K7* was notably higher in buckwheat seedlings from the Hap1 group compared to those from the Hap3 group (Figure 2f). The impact of base variation on promoter activity was further assessed by cloning the promoter regions of the two haplotypes (-2000 to -1700 bp) into the *pGreenII-0800-LUC* vector, which showed significantly higher activity for the Hap1 promoter than for Hap3 (Figure 2g). This indicates that differences in promoter activity between these two haplotypes influence *FtUGT71K7* expression. Additionally, G-box, W-box, and MYB binding sites are abundant in the *UGT71* promoter (Table S4), suggesting that the *UGT71* subfamily in buckwheat may be regulated by bHLH (Hao et al. 2021), WRKY (Jiang et al. 2017), and MYB (Liu, Osbourn, and Ma 2015) transcription factor families. These regulatory elements likely contribute to the observed variations in epicatechin content among different Tartary buckwheat haplotypes.

### 4.4 | Buckwheat Glycosyltransferase *FtUGT71K6* and *FtUGT71K7* Mediate UDP-Glucoside Transfer to Cyanidin and Epicatechin

Given the association of the *FtUGT71K* gene cluster with epicatechin, we hypothesised that these genes might facilitate the glycosylation of compounds in the epicatechin biosynthesis pathway. To test this hypothesis, we performed protein homology modelling for *FtUGT71K6* using Alphafold2-predicted A0A1P8SFY7.1.A as a template with 77.7% sequence

identity and over 30% concordance, meeting the requirements for modelling.

Previous studies have demonstrated that the *UGT71* subfamily in strawberries catalyses glycosyl transfer using anthocyanins as substrates (Song et al. 2015). Based on this, cyanidin and epicatechin were selected as substrates for molecular docking with *FtUGT71K6*. The docking results revealed that the glycosyl donor UDP-glucoside and the acceptors cyanidin and epicatechin were spatially proximate within the protein model, facilitating efficient reaction (Figure 3a,b). Specifically, UDP-glucoside formed a hydrogen bond with His-168 and hydrophobic interactions with Asn-172 in the PSG box (HCGWNS) of *FtUGT71K6*. Additionally, Gln-52 and Glu-176 interacted with all three substrates, highlighting the importance of these four sites for the catalytic activity of *FtUGT71K6*. The binding energies of the substrates to *FtUGT71K6* were all negative, suggesting that the catalytic reaction occurs spontaneously without the need for external energy (Figure 3c–e). UHPLC/MS analysis verified that *FtUGT71K6*-myc and *FtUGT71K7*-myc catalysed the formation of cyanidin-3-*O*-glucoside (Figure 3f–h) and also utilised epicatechin as a substrate for reaction (Figure 3i–k). These findings indicate that *FtUGT71K6* and *FtUGT71K7* proteins share similar catalytic functions, facilitating glycosylation of both epicatechin and cyanidin.

### 4.5 | Functional Validation of *FtUGT71K6* and *FtUGT71K7* in Epicatechin Biosynthesis and Metabolite Accumulation

To determine where *FtUGT71K6* and *FtUGT71K7* proteins function within the cell, subcellular localisation was performed in tobacco leaves and identified *FtUGT71K6* and *FtUGT71K7* localised to the cytoplasm and nucleus, respectively (Figure 4a). The subcellular localisation of flavonoid synthesis-related proteins is usually located in the nucleus and cytoplasm of the cell (Yang et al. 2022; Chen et al. 2024). To validate the role of *FtUGT71K6* and *FtUGT71K7* in the epicatechin biosynthesis pathway, we generated transgenic buckwheat hairy root and *Arabidopsis* lines (Figures 4b,c, S5). Overexpression of *FtUGT71K6* or *FtUGT71K7* in both hairy roots and *Arabidopsis* resulted in significantly increased levels of cyanidin-3-*O*-glucoside and epicatechin, confirming their involvements in the epicatechin biosynthesis pathway. In *FtUGT71K6*-OE and *FtUGT71K7*-OE hairy roots, procyanidin C1 and B1 levels also rose, while cyanidin and kaempferol levels were significantly decreased (Figure 4d), suggesting that kaempferol and epicatechin compete for the intermediate compound dihydrokaempferol and that procyanidins are downstream metabolites of the epicatechin synthesis pathway (Figure 4e). These results demonstrated that overexpression of *FtUGT71K6* or *FtUGT71K7* alters metabolite levels in the epicatechin synthesis pathway in *Arabidopsis* and hairy roots, promoting the accumulation of downstream compounds of this pathway.

Remarkably, this alteration in metabolite flow did not significantly affect plant growth, as *FtUGT71K6*-OE, *FtUGT71K7*-OE, and wild-type (WT) *Arabidopsis* plants exhibited similar growth under normal conditions (Supporting Information S1: Figure S6). However, total flavonoid content was significantly higher in

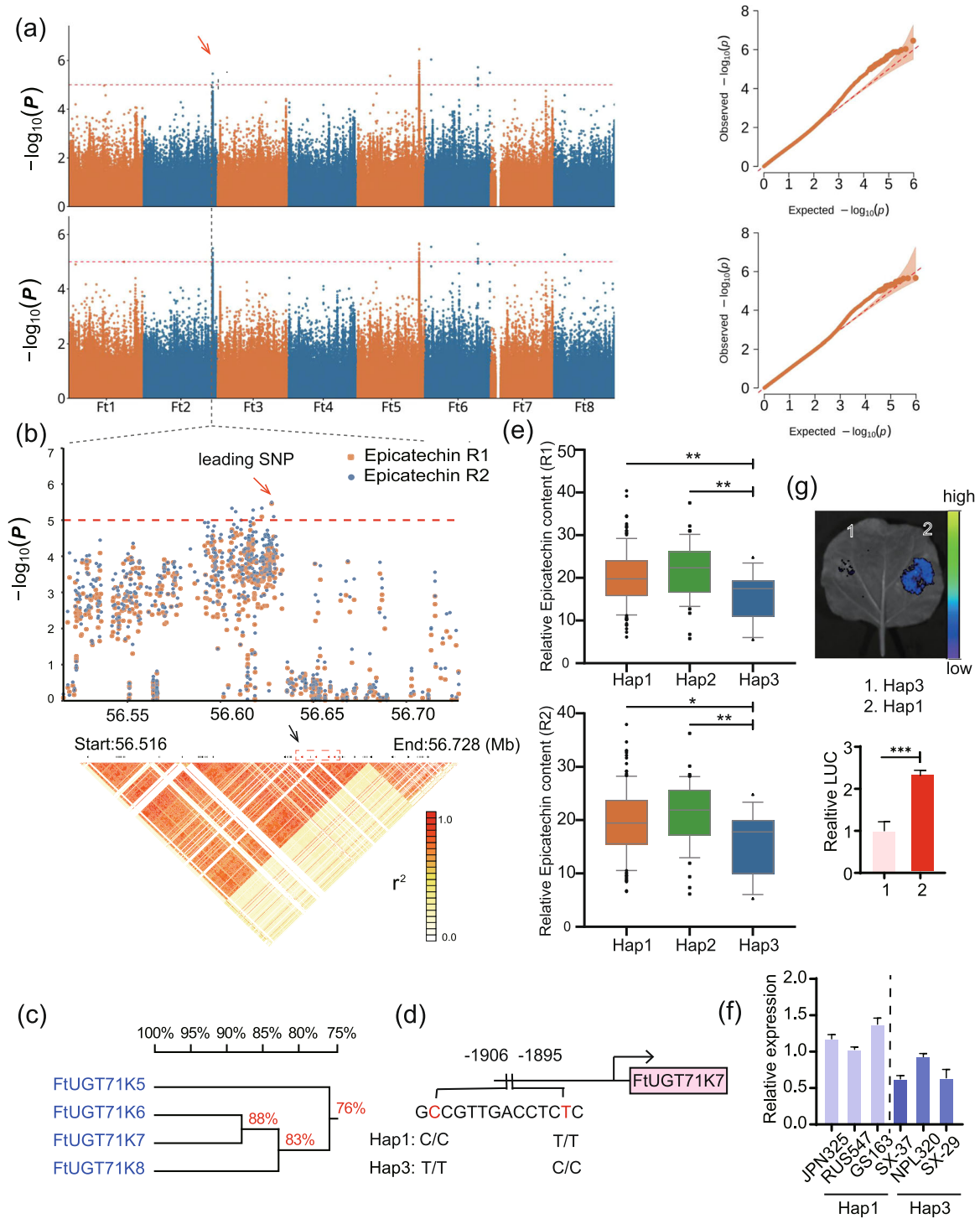


**FIGURE 2** | GWAS results of *FtUGT71K5*, *FtUGT71K6*, *FtUGT71K7*, and *FtUGT71K8* tandem repeat genes related with the content of epicatechin in 200 accessions of Tartary buckwheat. (a) Manhattan plot illustrating the GWAS result of Epicatechin content. GWAS had two repeats (left) and signal Significance Analysis (right). (b) Regional Manhattan Map. The 0.2 Mb genomic regions on either side of the most significant SNP. The lead SNP is shown with a red arrow. The tandem repeats were shown by the black arrow. (c) The protein similarity of *UGT71K* tandem repeats. (d) Haplotype located in the *FtUGT71K7* promoter. (e) The epicatechin content in 3 haplotypes in two biological replicates. Numbers of Hap1 is 140, Hap2 is 42, and Hap3 is 15. (f) Relative expression of *FtUGT71K7* in the Hap1 and Hap3 of Tartary buckwheat germplasm. (g) Identification of the activity of the *FtUGT71K7* promoter in Hap1 and Hap3 of Tartary buckwheat germplasm. Data are shown as mean  $\pm$  SD from three biological replicates ( $n = 5$ ). \* $p < 0.05$ , \*\* $p < 0.01$ , and \*\*\* $p < 0.001$ , significant different analysis based on two-tailed Student's *t*-test. [Color figure can be viewed at [wileyonlinelibrary.com](https://onlinelibrary.wiley.com)]

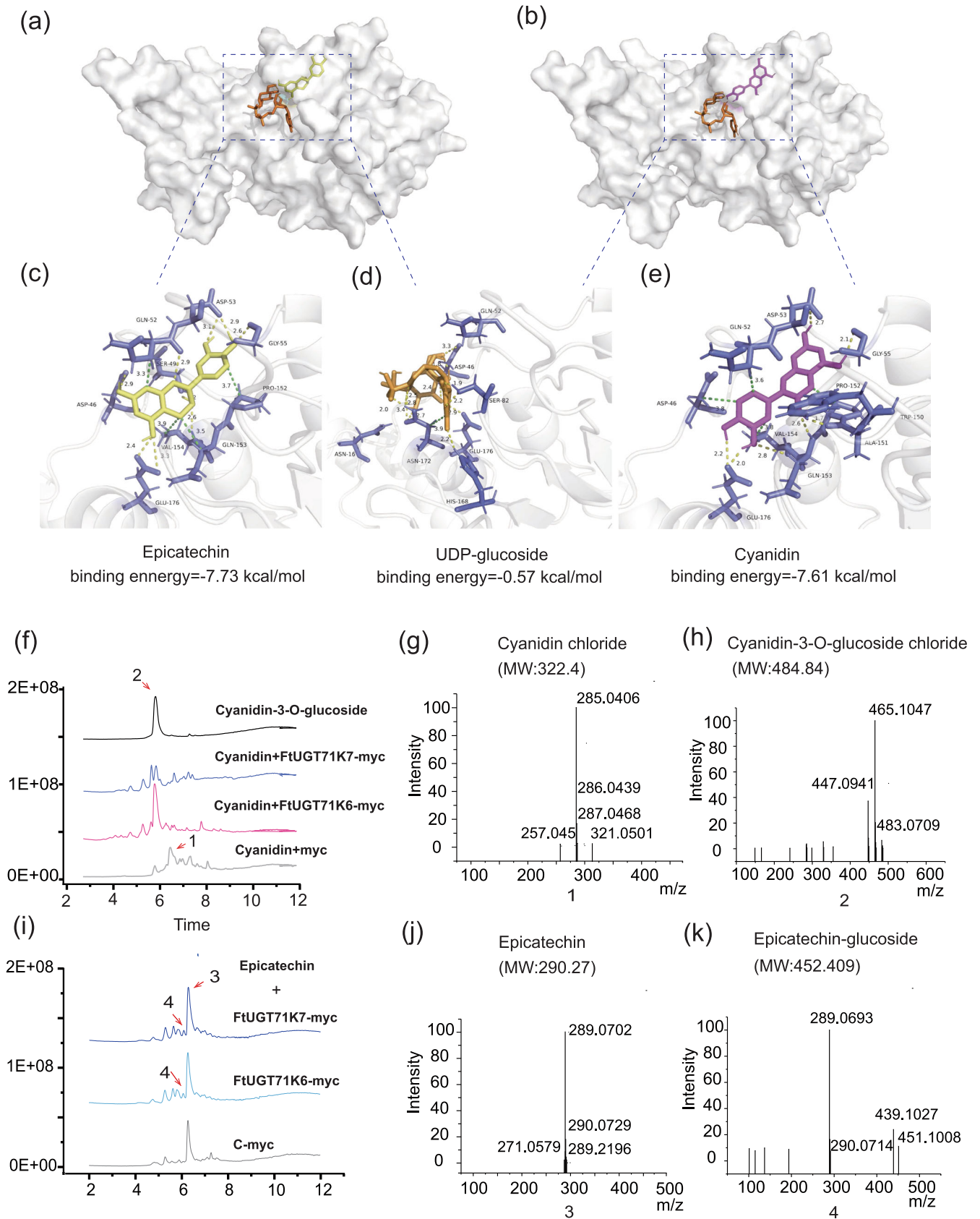


**FIGURE 3** | Legend on next page.

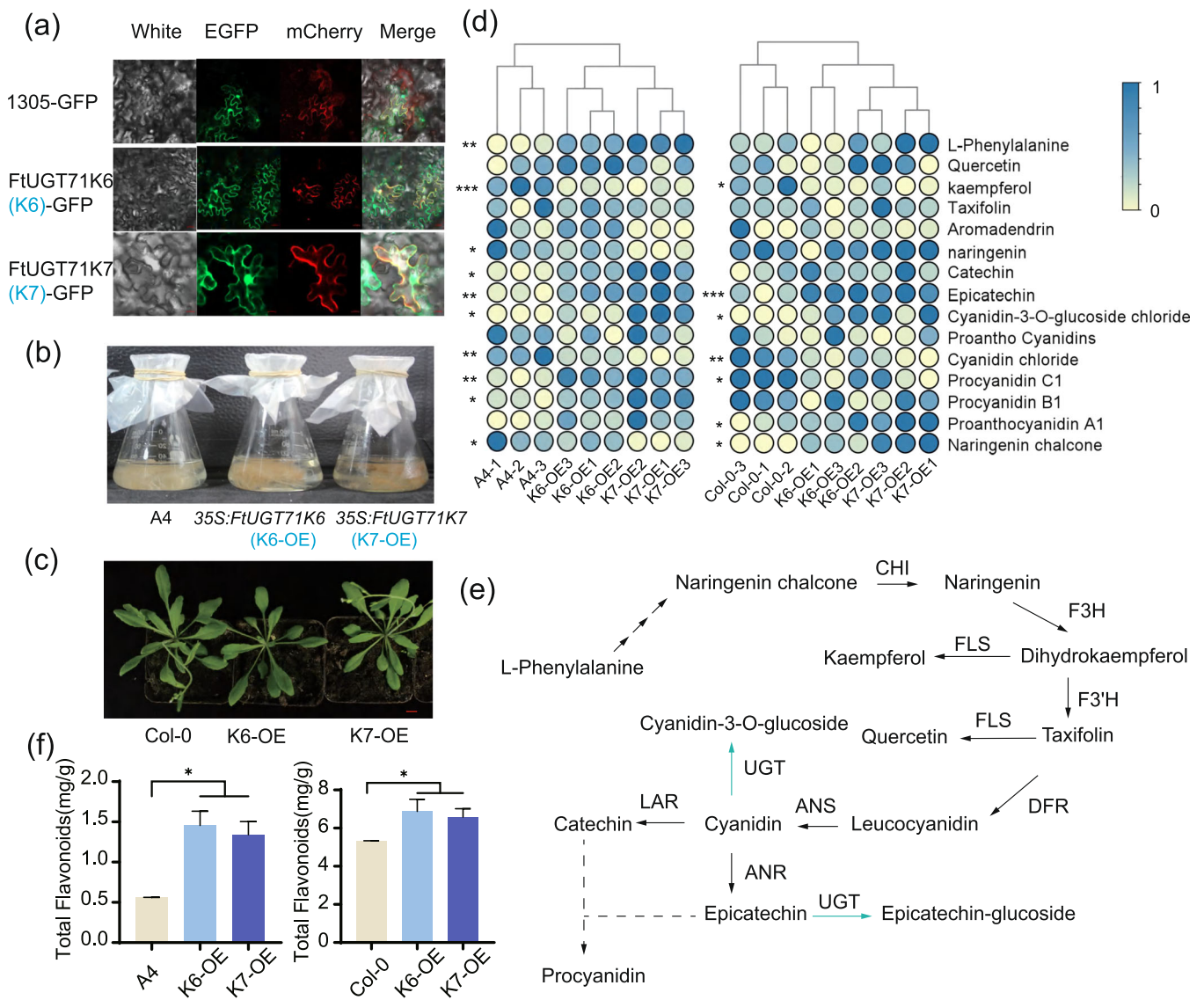


**FIGURE 4** | Overexpressed *FtUGT71K6* and *FtUGT71K7* in buckwheat hairy root and *Arabidopsis* influencing contents of compounds in epicatechin synthesis pathway. (a) Subcellular localisation of *FtUGT71K6* and *FtUGT71K7*. (b) Overexpressed hairy root. A4 as the control, K6-OE (*FtUGT71K6*-OE), K7-OE (*FtUGT71K7*-OE). (c) Overexpressed *Arabidopsis*. Wild type *Arabidopsis* (WT) as control, K6-OE (*FtUGT71K6*-OE), K7-OE (*FtUGT71K7*-OE). (d) Heatmap displaying the compounds content about the epicatechin synthesis pathway in K6-OE and K7-OE overexpressed buckwheat hairy roots (left), overexpressed *Arabidopsis* (right). The data treated with min-max normalisation, A4 as the control in hairy root, Col-0 as the control in *Arabidopsis*, and the contents of compounds in K6-OE or K7-OE were uniformly analyzed by the student's *t*-test; each line has three biological repeats \**p* < 0.05, \*\**p* < 0.01 and \*\*\**p* < 0.001. (e) Epicatechin biosynthesis pathway. CHI, chalcone isomerase; F3H, flavanone 3-hydroxylase; F3'H, flavonoid 3'-hydroxylase; FLS, flavonol synthase; DFR, dihydroflavonol-4-reductase; ANS, anthocyanidin synthase; ANR, anthocyanidin reductase; LAR, Leucoanthocyanidin reductase; UGT, glycosyltransferase. (f) Total flavonoids in K6-OE and K7-OE buckwheat hairy roots (left), K6-OE and K7-OE *Arabidopsis* (right). Each line contains three biological repeats. \**p* < 0.05 (one-way ANOVA, Tukey's post-test). [Color figure can be viewed at [wileyonlinelibrary.com](https://onlinelibrary.wiley.com)]

**FIGURE 3** | *FtUGT71K6* and *FtUGT71K7* catalyse the glycosylation of epicatechin and cyanidin. (a) The map of donor UDP-glucoside and receptor epicatechin autodocking with UGT71K6 protein. (b) UDP-glucoside and cyanidin autodocking with UGT71K6 protein. (c) Detailed presentation of the UGT71K6 protein and epicatechin binding site. (d) Detailed information about UDP-glucoside binding with protein. (e) Detailed information about cyanidin binding with protein. Site selection is based on the design of sites that require less binding energy and the possibility of spatial binding of donor and acceptor. Yellow dashed lines indicate hydrogen bonds. The green dashed line indicates hydrophobic interactions, and the data on the side indicate bond distances (Å). (f) UPLC analysis of reaction products from cyanidin. C-myc protein as the control, *FtUGT71K6*-myc and *FtUGT71K7*-myc extract from overexpressed hairy root, purified by myc-beads. 1. the peak of cyanidin; 2. the product peak from cyanidin and *FtUGT71K6*. (g and h) Specific mass spectrometry in (f), electrospray ionisation is performed in negative ion mode. (i) UHPLC analysis of reaction products from epicatechin. *FtUGT71K6*-myc and *FtUGT71K7*-myc extract from overexpressed hairy root, purified by myc-beads. (j and k) Specific mass spectrometry in (i), electrospray ionisation is performed in negative ion mode. 3. the peak of epicatechin; 4. the product peak from epicatechin and *FtUGT71K6* and *FtUGT71K7*. [Color figure can be viewed at [wileyonlinelibrary.com](https://onlinelibrary.wiley.com)]

*FtUGT71K6*-OE and *FtUGT71K7*-OE (Figure 4f), indicating that overexpression of *FtUGT71K6* or *FtUGT71K7* enhances the accumulation of epicatechin and cyanidin-3-*O*-glucoside in plants, thereby increasing total flavonoid contents without affecting plant growth.

#### 4.6 | *FtUGT71K6* and *FtUGT71K7* Enhance Drought Tolerance

UGT family genes are known to contribute to abiotic and biotic stress resilience (Dong et al. 2020; Zhang, Sun, et al. 2021; Gharabli, Della Gala, and Welner 2023). Flavonoids, synthesised via UGT pathways, are recognised for their role in enhancing plant antioxidant capacity (Di Ferdinando et al. 2012). To assess the role of *FtUGT71K6* and *FtUGT71K7* in drought tolerance, we evaluated the drought resistance of *FtUGT71K6*-OE and *FtUGT71K7*-OE. Under non-stressed conditions, no differences were observed in the growth status of *FtUGT71K6*-OE and *FtUGT71K7*-OE compared to the wild type (Supporting Information S1: Figures S6 and S7). However, under drought stress, the root length (cultured in MS medium) or above-ground biomass (cultured in soil) of *FtUGT71K6*-OE and *FtUGT71K7*-OE *Arabidopsis* were significantly higher than those of controls (Figures 5a,b, and S7). Under PEG treatment, the fresh weight of *FtUGT71K6*-OE and *FtUGT71K7*-OE hairy roots was approximately 3.1 and 1.57 times that of the A4 control, respectively (Figure 5c,d).

To further investigate the mechanisms underlying the observed drought tolerance, we measured various physiological indicators. DAB and NBT staining in *Arabidopsis* detected hydrogen peroxide (H<sub>2</sub>O<sub>2</sub>) and superoxide levels, respectively. Results revealed that *FtUGT71K6*-OE and *FtUGT71K7*-OE *Arabidopsis* exhibited lighter staining under drought conditions, indicating enhanced reactive oxygen species (ROS) scavenging ability (Figures 5e and S8). Additionally, malondialdehyde (MDA) content, an indicator of lipid peroxidation in plants, was significantly lower in overexpressed *Arabidopsis* and hairy roots, indicating less stress-induced plant damage compared to controls (Figure 5f,g). Conversely, antioxidant enzyme activities (SOD, CAT and POD), proline, and soluble sugar content were significantly decreased in the transgenic lines (Supporting Information S1: Figure S9), suggesting that the observed ROS scavenging ability might not be directly linked to increased antioxidant enzyme activity. Additionally, the content of cyanidin-3-*O*-glucoside and procyanidins significantly increased in *FtUGT71K6*-OE and *FtUGT71K7*-OE under drought stress (Figure 5h). *FtUGT71K6*-OE or *FtUGT71K7*-OE showed higher total antioxidant capacity, whether stressed or not (Figure 5i). These findings suggest that this altered metabolite profile in *FtUGT71K6*-OE and *FtUGT71K7*-OE enhanced plant antioxidants, ultimately improving drought tolerance.

#### 4.7 | *FtUGT71K6*-OE Has a Positive Effect on Salinity Tolerance, but Neither *FtUGT71K6*-OE nor *FtUGT71K7*-OE Responds to *Rhizoctonia solani* AG4-HGI 3

The accumulation of flavonoids is known to enhance antioxidant capacity, which often increases plant resilience to

various stresses (Gharabli, Della Gala, and Welner 2023). Therefore, we analyzed *FtUGT71K6*-OE and *FtUGT71K7*-OE for salt tolerance and disease resistance. Under salt stress, *FtUGT71K7*-OE *Arabidopsis* did not exhibit significant changes in root length. In contrast, we found that *FtUGT71K6*-OE hairy roots and *Arabidopsis* plants demonstrated notable improvements in salt tolerance compared to wild-type controls. However, the overexpressed hairy roots did not show an increase in antioxidant enzyme activity or osmoregulatory substances (Supporting Information S1: Figures S10, S11, S12). The MDA content in *FtUGT71K6*-OE was lower than in controls, indicating that *FtUGT71K6* overexpression can mitigate plant peroxide damage under salt stress (Supporting Information S1: Figure S12). Furthermore, *FtUGT71K6*-OE showed a higher total antioxidant capacity compared to the control (Supporting Information S1: Figure S11), which may explain the lower MDA levels observed. Under salt stress, *FtUGT71K6*-OE hairy roots also displayed significantly elevated levels of cyanidin-3-*O*-glucoside and procyanidin A1 compared to controls, both of which are potent antioxidants (Supporting Information S1: Figure S13). Therefore, we concluded that increased levels of cyanidin-3-*O*-glucoside and procyanidin A1 likely enhance total antioxidant capacity and reduce oxidative damage in *FtUGT71K6*-OE buckwheat hairy roots.

In terms of disease resistance, *FtUGT71K6*-OE and *FtUGT71K7*-OE did not exhibit significant resistance to *Rhizoctonia solani* infection (Supporting Information S1: Figure S14), suggesting that the metabolite changes in *FtUGT71K6*-OE and *FtUGT71K7*-OE do not significantly influence pathogen tolerance.

#### 4.8 | Positive Selection Sites in *FtUGT71K6* and *FtUGT71K7*: GLN-34, ASP-53 and ILE-266

Gene duplication is proposed as a primary mechanism driving the evolution of UGT family genes (Erthmann, Agerbirk, and Bak 2018; Yang et al. 2024). We hypothesised that positive selection might have influenced the evolution of the *UGT71K5*, *UGT71K6*, *UGT71K7*, and *UGT71K8* gene cluster. Therefore, we analyzed evolutionary selection pressures on the *UGT71K5*, *UGT71K6*, *UGT71K7*, and *UGT71K8* tandem repeat genes. The *FtUGT71K5*, *FtUGT71K6*, *FtUGT71K7*, and *FtUGT71K8* cluster, located on the distal end of chromosome 2, is conserved across *F. dibotrys*, *F. esculentum*, and *F. tataricum*. Notably, there are no gene insertions within the *UGT71K* tandem duplication region in *F. esculentum* and *F. tataricum*, although a 254-bp sequence between *FtUGT71K5* and *FtUGT71K6*, resembling a *UGT71K* sequence, may function as a pseudogene. Additionally, a short sequence is found upstream of the *FeUGT71K5* gene in *F. esculentum* (Figure 6a). Sequence conservation analysis of *UGT71K5*, *UGT71K6*, *UGT71K7*, and *UGT71K8* in buckwheat revealed similarity levels exceeding 77%, leading to the construction of a homology tree that divided these sequences into three distinct branches (Figure 6b).

Based on the influence of selection pressure on tandem repeat genes (Erthmann, Agerbirk, and Bak 2018), we conducted selection pressure analysis on *UGT71K5*, *UGT71K6*, *UGT71K7*, and *UGT71K8* sequences from *F. dibotrys*, *F. esculentum*, and *F. tataricum* using the Branch-Site model. The log-likelihood ratio

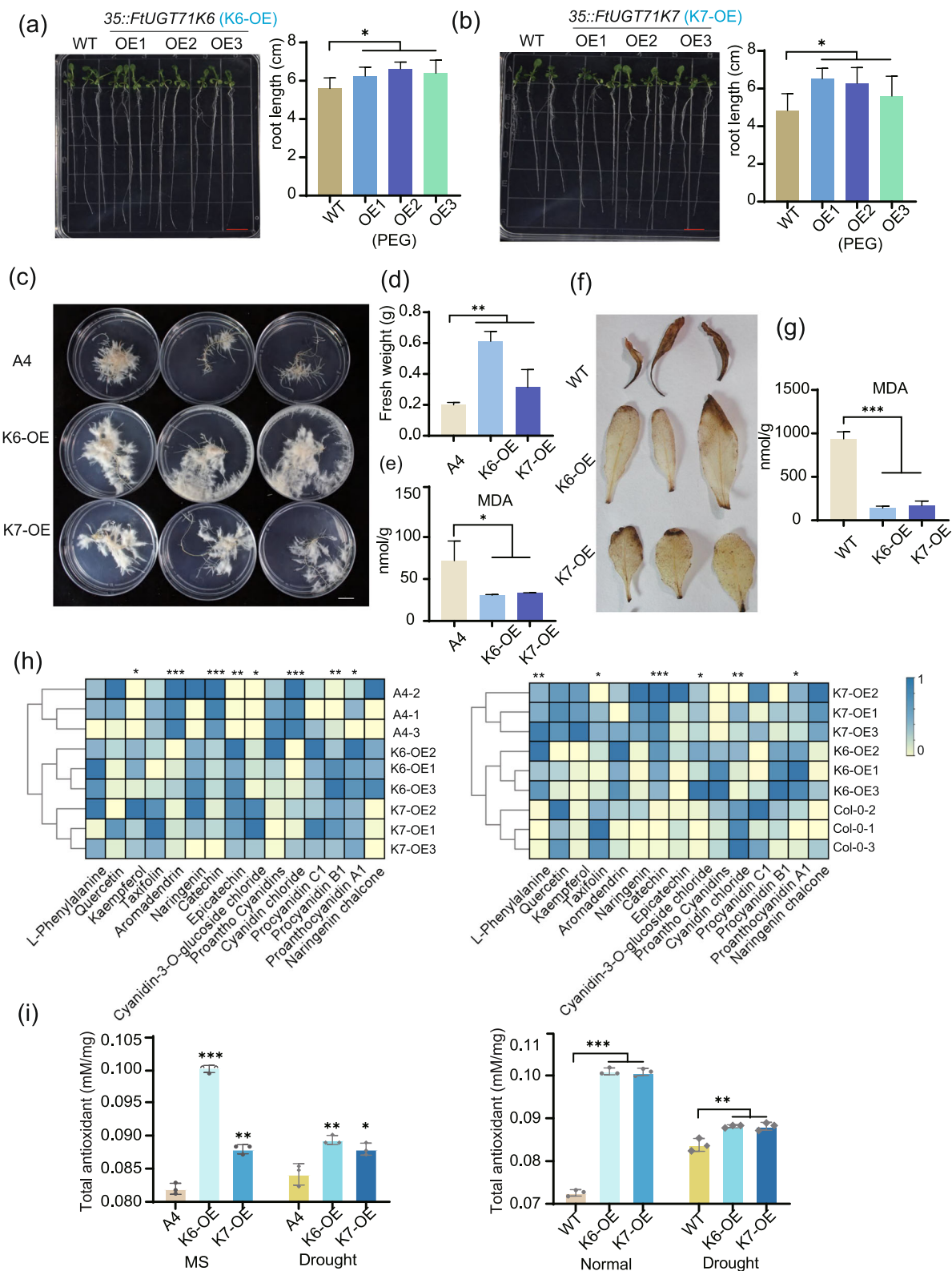


**FIGURE 5** | Phenotype of drought-tolerant overexpressed *FtUGT71K6* and *FtUGT71K7* *Arabidopsis* and buckwheat hairy roots. (a) K6-OE (*FtUGT71K6*-OE) treated with 10% PEG 7 days (left), root length measurement (right). (b) K7-OE (*FtUGT71K7*-OE) treated with 10% PEG 7 days. (c) 10% PEG-treated K6-OE and K7-OE hairy roots for 14 days in MS medium. (d) Fresh weight of (c). (e) DAB staining. *Arabidopsis* grown in soil for 21 days with a cessation of watering. (f) MDA content in *FtUGT71K6*-OE and *FtUGT71K7*-OE hairy roots. (g) MDA content in *FtUGT71K6*-OE and *FtUGT71K7*-OE *Arabidopsis*. The values are means  $\pm$  SD ( $n = 3$  biological replicates). \* $p < 0.05$ , \*\* $p < 0.01$ , \*\*\* $p < 0.001$  one-way ANOVA, Tukey's post-test was used to calculate the significant differences relative to the control. (h) The contents of compounds in the epicatechin synthesis pathway. Each line has three biological replicates ( $n = 3$ ). Min-Max Normalisation was used in the heat map. (i) Total antioxidant capacity of *FtUGT71K6*-OE and *FtUGT71K7*-OE overexpressed hairy roots (left) and overexpressed *Arabidopsis* (right). \* $p < 0.05$ , \*\* $p < 0.01$ , significant differences analysis based on two-tailed Student's *t*-test. [Color figure can be viewed at [wileyonlinelibrary.com](https://onlinelibrary.wiley.com)]

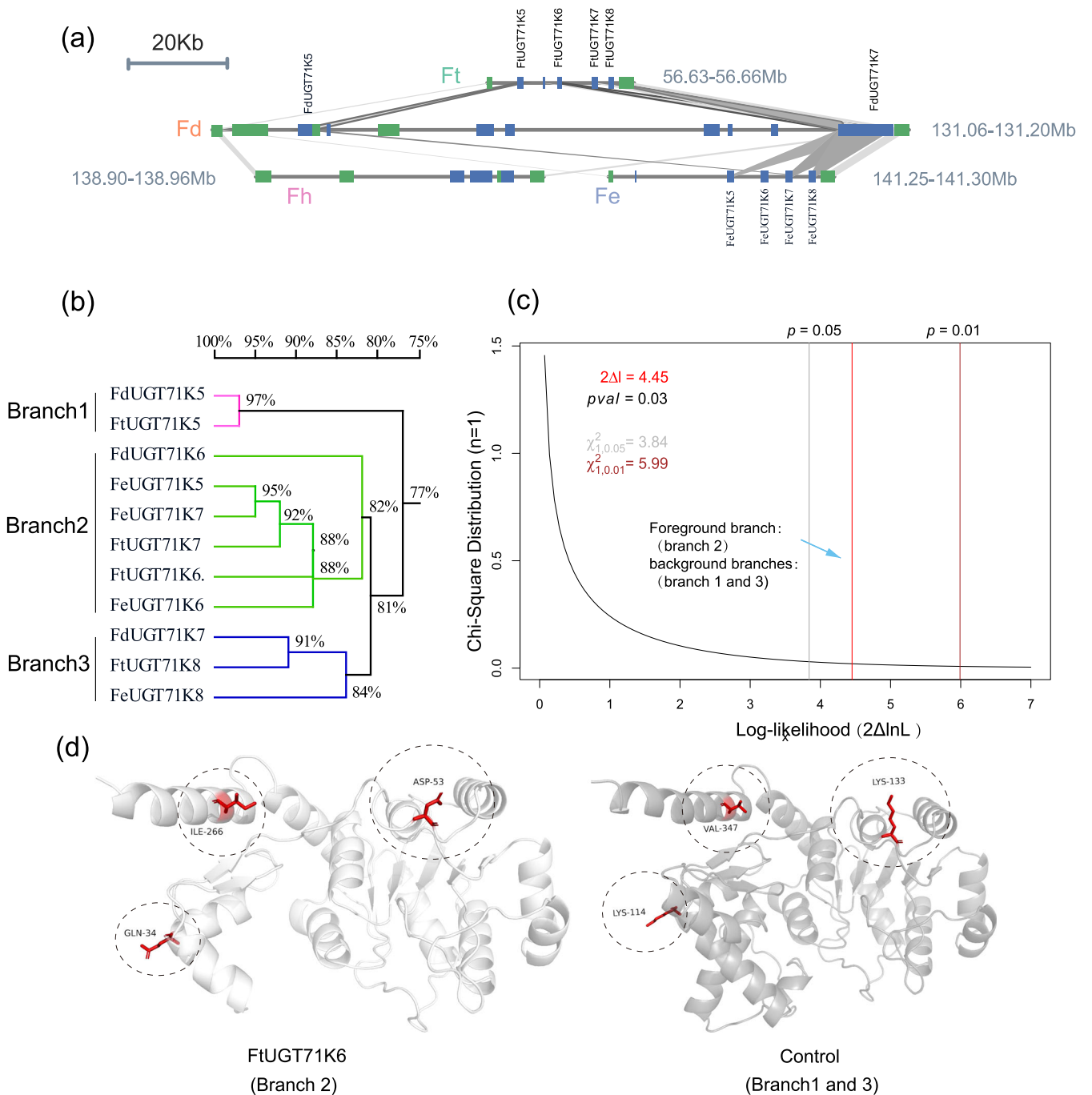


**FIGURE 6** | Selection pressure analysis of *UGT71K5*, *UGT71K6*, *UGT71K7*, and *UGT71K8* tandem repeats in buckwheat. (a) Detailed map of *UGT71K5*, *UGT71K6*, *UGT71K7*, and *UGT71K8* genomic regions. (b) *UGT71K5*, *UGT71K6*, *UGT71K7*, and *UGT71K8* homology tree. (c) Branch site model selection pressure analysis. The grey line represents  $2\Delta l = 3.84$ ,  $p = 0.05$ , and the dark red line represents  $p = 0.01$ ,  $2\Delta l = 5.99$ . The red line represents  $2\Delta l = 4.45$ ,  $p = 0.03$ , computed by branch 2 as the foreground branch 1 and 3 as the background branches. (d) Visualisation of positively selected amino acid sites. The model of the control was built with FtUGT71K5 (belonging to branch 2), whose template was consistent with that of the experimental group, while the model consistency was 100%. [Color figure can be viewed at [wileyonlinelibrary.com](https://onlinelibrary.wiley.com)]

test between models yielded a value of 4.45 with a  $p$ -value of 0.03 (Figure 6c), suggesting significant positive selection on genes in branch 2, as compared to background branches 1 and 3 (Figure 6c). The results indicated that FtUGT71K6, FtUGT71K7, and other branch 2 proteins with GLN-34, ASP-53, and ILE-266 may have been positively selected compared to branch 1 and 3 counterparts, which have LYS-114, LYS-133, and VAL-347 at corresponding positions (Figure 6d).

## 5 | Discussions

The *UGT71* subfamily represents a large glycosyltransferase gene family in the buckwheat genome (Yang et al. 2024). Genes within the buckwheat *UGT71* subfamily, which share over 75% similarity with *Arabidopsis UGT71* genes, were identified based on the conserved structural domain of glycosyltransferase (Supporting Information S2: Table S1, Supporting Information

S1: Figure S1). The *UGT* gene family often exists as tandem duplication in plant genomes (Kuzina et al. 2011), and covariance analysis suggested that the *UGT71* subfamily is positionally conserved with tandem duplications in the buckwheat genome (Supporting Information S1: Figure S3). The *FtUGT71K5*, *FtUGT71K6*, *FtUGT71K7*, and *FtUGT71K8* gene cluster gained our attention due to its location within a region highly correlated with epicatechin content in Tartary Buckwheat, as identified by GWAS (Figure 2a), and eventually this gene cluster was found to be associated with epicatechin content (Figure 2b).

Catechin and epicatechin are the most abundant bound phenolic compounds formed when buckwheat seeds are processed into flour (Martín-García et al. 2019). To further understand the influence of tandem gene duplications on epicatechin content across various buckwheat germplasms, we performed a haplotype analysis of the *FtUGT71K7* promoter. Hap1, which correlates with higher epicatechin content, constitutes a significant proportion of the 200 Tartary buckwheat accessions (Figure 2e), suggesting it may have undergone a subtle selection process. And only two bases difference in Hap1 enhances the promoter activity and expression level of *FtUGT71K7* compared to Hap3 (Figure 2g,f). Interestingly, this 14-bp haplotype's sequence 5'-GCCGTTGACCTCTC-3' contains the W-box core sequence (TGACCA/T), crucial for WRKY transcription factor binding (Lim et al. 2022). Therefore, the variations in epicatechin content among haplotypes may be associated with WRKY transcription factors.

Plant glycosyltransferases exhibit multi-substrate catalytic functions (Cui et al. 2016). For instance, UGT71 subfamily members in strawberries catalyse reactions using flavonoids as substrates, with unique properties depending on the sequence (Song et al. 2015). In buckwheat, we localised the *FtUGT71K6*, *FtUGT71K7* gene cluster using GWAS data and demonstrated their role in influencing epicatechin synthesis in both in vivo and in vitro (Figures 2, 3, and 4). GWAS data also indicated that the genomic region of *FtUGT71K6*, *FtUGT71K7* corresponds to procyanidin A3 and epicatechin-epiafzelechin content (Supporting Information S1: Figure S4). Procyanidin A3 is a polymer formed with epicatechin monomers and is a part of the proanthocyanidin (PA) pathway (Debeaujon et al. 2003), where TT12 is a membrane protein involved in proanthocyanidin (PA) synthesis and facilitates the accumulation of procyanidins in vesicles (Debeaujon et al. 2001). TT12 transports cyanidin-3-*O*-glucoside but not catechin-3-*O*-glucoside and does not translocate free cyanidin or epicatechin directly into vesicles (Marinova et al. 2007). Rather, the glycosylated form of epicatechin is potentially transported by TT2 to vesicles, either as a precursor cyanidin or as cyanidin glycosylated form, which then undergoes hydrolysis for subsequent polymerisation reactions for PA synthesis (Marinova et al. 2007; Zhao and Dixon 2010). Thus, the association of *FtUGT71K5*, *FtUGT71K6*, *FtUGT71K7*, and *FtUGT71K8* with procyanidin A3 content in the GWAS data suggests that these genes may influence procyanidin A3 levels. Although *FtUGT71K6* and *FtUGT71K7* utilised both cyanidin and epicatechin as substrates, their overexpression lines exhibited increased epicatechin content, consistent with the general multi-substrate catalytic nature of glycosyltransferases (Xu et al. 2021; Ren et al. 2023), which may have complex

effects on the compound content across the entire metabolic pathway. Overexpression of *FtUGT71K6* and *FtUGT71K7* led to increased epicatechin and procyanidin accumulation while reducing cyanidin levels, likely due to the need to replenish epicatechin (Figure 4). Though overexpression of *FtUGT71K6* or *FtUGT71K7* in plant species affects the flow of metabolites, it enhances the total flavonoid content in the plant (Figure 4). Overexpression of glycosyltransferases has been shown to promote flavonoid accumulation. For example, overexpression of the glycosyltransferase *UGT71C4* enhanced the enrichment of several flavonoids (Cao et al. 2024).

Plants employ antioxidant mechanisms like increased enzyme activity (Gechev et al. 2003), flavonoid and procyanidin accumulation (Ahmed et al. 2021), and osmotic adjustment (Mahmood et al. 2020) to counter oxidative stress from abiotic and biotic sources. The specific antioxidant responses vary among plant species and stress type (Mahmood et al. 2020). Flavan-3-ols, anthocyanidins, and procyanidins are examples of potent antioxidants (Youn et al. 2006; Khan and Abbas 2023; Zhao, Jiang, et al. 2023). In the context of drought tolerance, *FtUGT71K6*-OE and *FtUGT71K7*-OE enhance the levels of procyanidins and anthocyanins, while DAB and NBT staining showed lower accumulation of hydrogen peroxide and superoxide (Figures 5, S8). The activities of SOD, POD, CAT, and the levels of proline and soluble sugar in the overexpressed lines were all lower compared to controls under drought treatment (Supporting Information S1: Figures S8, S11). Typically, antioxidant enzyme activities and osmoregulatory substances are upregulated in response to stress (Ozturk et al. 2021; Iqbal et al. 2023). These results suggest that the overexpressing lines experienced less damage during drought treatment, resulting in lower antioxidant enzyme activity and osmoregulatory substance levels.

The antioxidant activity of flavan-3-ols and procyanidins results from phenolic hydroxyl groups stabilising free radicals, thereby reducing oxidative damage (Fraga et al. 2010; Verstraeten, Fraga, and Oteiza 2015). Therefore, we hypothesised that overexpression of *FtUGT71K6* or *FtUGT71K7* increases natural antioxidants, such as flavan-3-ols, that directly scavenge ROS, reducing oxidative stress. Consistent with this, *FtUGT71K6*-OE and *FtUGT71K7*-OE showed higher total antioxidant capacity than controls under normal and drought conditions (Figure 5i), indicating that overexpression of *FtUGT71K6* and *FtUGT71K7* in plants improves antioxidant capacity and reduces oxidative stress.

Distinct steady-state levels of ROS in various cellular compartments (e.g., chloroplasts, peroxisomes, mitochondria, cytoplasm, nuclei) collectively contribute to an overall ROS signature that reflects cellular redox status. Drought and salinity stress generate specific subcellular ROS and redox signatures and contribute to the signalling pathways that mediate their distinct stress responses (Choudhury et al. 2017). *FtUGT71K6*-OE *Arabidopsis* and hairy roots showed significant salt tolerance, while *FtUGT71K7*-OE *Arabidopsis* did not exhibit significant salt tolerance (Supporting Information S1: Figures S10, S11, S12). Differences in amino acids between the similar proteins *FtUGT71K6* and *FtUGT71K7* (Figure 6) may explain their functional discrepancies, as reflected in the

varying flavonoid content between *FtUGT71K6*-OE and *FtUGT71K7*-OE (Figure 4d). The level of accumulated antioxidants affects the ROS scavenging capacity by phenolic hydroxyl groups that stabilise free radicals (Martinez et al. 2016; Ma et al. 2022). We therefore hypothesised that the contrasting phenotypes of *FtUGT71K6*-OE and *FtUGT71K7*-OE under salt stress might be related to antioxidant accumulation. Although fungal infestation can influence flavonoid levels, osmoregulators, and antioxidant enzyme activity (Chen et al. 2023; Zhang, Feng, et al. 2023), we did not observe significant disease resistance in *FtUGT71K6*-OE and *FtUGT71K7*-OE *Arabidopsis* (Supporting Information S1: Figure S14). Therefore, we speculate that the minor metabolite changes observed are insufficient to confer disease resistance.

Tandem gene duplications contribute to genome evolution by altering gene regulation and optimising biosynthetic pathways (Zhang et al. 2024). Differences among duplicated genes can lead to altered enzyme functions (Copley 2020). Gene family analysis showed that *UGT71K5*, *UGT71K6*, *UGT71K7*, and *UGT71K8* tandem duplications are conserved across multiple buckwheat species (Figure 2). The neighbouring genes to *FtUGT71K6* and *FtUGT71K7* exhibit similar expression patterns (Figures 1 and S2). According to GWAS analysis and functional validation, *FtUGT71K6* and *FtUGT71K7* tandem duplication genes are functionally similar (Figures 2, 3, 4, and 5). However, there are still discrepancies in the amino acid sequences of *UGT71K5*, *UGT71K6*, *UGT71K7*, and *UGT71K8* (Supporting Information S1: Figures S1 and 6b). Functional divergence and altered functional constraints on amino acid residues after gene duplication may contribute to their distinct functions (Wu et al. 2019). Selection pressure analysis identified LYS-114, LYS-133 and VAL-347 as three potential sites of evolutionary selection (Figure 6c,d). Remarkably, ASP-53 has been previously identified as a key site for substrate binding based on molecular docking studies (Figure 3), and changes at these key amino acid sites lead to altered catalytic function (Xu et al. 2021). We therefore believe that the change of key amino acids largely contributes to differences in the catalytic function of *FtUGT71K5*, *FtUGT71K6*, *FtUGT71K7*, and *FtUGT71K8*.

Taken together, our findings suggest that *FtUGT71K6* and *FtUGT71K7* are present as tandem duplicates in the buckwheat genome and exhibit evolutionary selection pressure by gene family analysis and detection of selection pressure. GWAS results of epicatechin and functional studies of *FtUGT71K6* and *FtUGT71K7* demonstrate that overexpression of these tandem duplicate genes enhances the total antioxidant capacity of the plant by altering the flow of metabolites in the epicatechin synthesis pathway, thereby improving drought tolerance. The results provide key candidate genes of the *UGT71* subfamily for future molecular breeding of abiotic stress resistance and potential metabolic engineering of flavonoid compounds of buckwheat and its related species.

## Acknowledgements

This research was supported by National Key Research and Development Program of China (2022YFE0140800) and the National Natural Science Foundation of China (32161143005).

## Conflicts of Interest

The authors declare no conflicts of interest.

## Data Availability Statement

The transcriptome sequencing data of *Fagopyrum tataricum*, *Fagopyrum esculentum* var. *homotropicum*, *Fagopyrum esculentum*, and *Fagopyrum dibotrys* were downloaded from the China National Center of Bioinformatics (CNCB) with the accession number (PRJCA009421), (PRJCA010349), (PRJCA009237), (PRJCA009421), respectively (He et al. 2022; He et al. 2023a; Zhang, He, et al. 2023; Zhang et al. 2017).

## References

- Ahmed, U., M. J. Rao, C. Qi, et al. 2021. "Expression Profiling of Flavonoid Biosynthesis Genes and Secondary Metabolites Accumulation in *Populus* Under Drought Stress." *Molecules* 26: 5546.
- Birchler, J. A., and H. Yang. 2022. "The Multiple Fates of Gene Duplications: Deletion, Hypofunctionalization, Subfunctionalization, Neofunctionalization, Dosage Balance Constraints, and Neutral Variation." *Plant Cell* 34: 2466–2474.
- Bönisch, F., J. Frotscher, S. Stanitzek, et al. 2014. "A UDP-Glucose: Monoterpenol Glucosyltransferase Adds to the Chemical Diversity of the Grapevine Metabolome." *Plant Physiology* 165: 561–581.
- Bowles, D., J. Isayenkova, E. K. Lim, and B. Poppenberger. 2005. "Glycosyltransferases: Managers of Small Molecules." *Current Opinion in Plant Biology* 8: 254–263.
- Bowles, D., E. K. Lim, B. Poppenberger, and F. E. Vaistij. 2006. "Glycosyltransferases of Lipophilic Small Molecules." *Annual Review of Plant Biology* 57: 567–597.
- Cao, G., E. Sofic, and R. L. Prior. 1997. "Antioxidant and Prooxidant Behavior of Flavonoids: Structure-Activity Relationships." *Free Radical Biology and Medicine* 22: 749–760.
- Cao, Y., Z. Han, Z. Zhang, et al. 2024. "UDP-Glucosyltransferase 71C4 Controls the Flux of Phenylpropanoid Metabolism to Shape Cotton Seed Development." *Plant Communications* 5: 100938.
- Caputi, L., M. Malnoy, V. Goremykin, S. Nikiforova, and S. Martens. 2012. "A Genome-Wide Phylogenetic Reconstruction of Family 1 UDP-Glycosyltransferases Revealed the Expansion of the Family During the Adaptation of Plants to Life on Land." *Plant Journal* 69: 1030–1042.
- Chen, L., Y. Yao, Y. Cui, et al. 2024. "Understanding the Molecular Regulation of Flavonoid 3'-hydroxylase in Anthocyanin Synthesis: Insights From Purple Qingke." *BMC Genomics* 25: 823.
- Chen, T., H. Cao, M. Wang, et al. 2023. "Integrated Transcriptome and Physiological Analysis Revealed Core Transcription Factors That Promote Flavonoid Biosynthesis in Apricot in Response to Pathogenic Fungal Infection." *Planta* 258: 64.
- Chen, T. H. H., and N. Murata. 2002. "Enhancement of Tolerance of Abiotic Stress by Metabolic Engineering of Betaines and Other Compatible Solutes." *Current Opinion in Plant Biology* 5: 250–257.
- Choudhury, F. K., R. M. Rivero, E. Blumwald, and R. Mittler. 2017. "Reactive Oxygen Species, Abiotic Stress and Stress Combination." *Plant Journal* 90: 856–867.
- Copley, S. D. 2020. "Evolution of New Enzymes by Gene Duplication and Divergence." *FEBS Journal* 287: 1262–1283.
- Cos, P., T. De Bruyne, N. Hermans, S. Apers, D. Berghe, and A. Vlietinck. 2004. "Proanthocyanidins in Health Care: Current and New Trends." *Current Medicinal Chemistry* 11: 1345–1359.
- Cui, L., S. Yao, X. Dai, et al. 2016. "Identification of UDP-Glycosyltransferases Involved in the Biosynthesis of Astringent Taste Compounds in Tea (*Camellia sinensis*)." *Journal of Experimental Botany* 67: 2285–2297.

- Debeaujon, I., N. Nesi, P. Perez, et al. 2003. "Proanthocyanidin-Accumulating Cells in *Arabidopsis testa*: Regulation of Differentiation and Role in Seed Development." *Plant Cell* 15: 2514–2531.
- Debeaujon, I., A. J. M. Peeters, K. M. Léon-Kloosterziel, and M. Koornneef. 2001. "The Transparent TESTA12Gene of *Arabidopsis* Encodes a Multidrug Secondary Transporter-Like Protein Required for Flavonoid Sequestration in Vacuoles of the Seed Coat Endothelium." *Plant Cell* 13: 853–871.
- Dong, N. Q., Y. Sun, T. Guo, et al. 2020. "UDP-Glucosyltransferase Regulates Grain Size and Abiotic Stress Tolerance Associated With Metabolic Flux Redirection in Rice." *Nature Communications* 11: 2629.
- Dong, T., Z. Y. Xu, Y. Park, D. H. Kim, Y. Lee, and I. Hwang. 2014. "Abscisic Acid Uridine Diphosphate Glucosyltransferases Play a Crucial Role in Abscisic Acid Homeostasis in *Arabidopsis*." *Plant Physiology* 165: 277–289.
- Du, Y. Y., P. C. Wang, J. Chen, and C. P. Song. 2008. "Comprehensive Functional Analysis of the Catalase Gene Family in *Arabidopsis thaliana*." *Journal of Integrative Plant Biology* 50: 1318–1326.
- Erthmann, P. Ø., N. Agerbirk, and S. Bak. 2018. "A Tandem Array of UDP-Glycosyltransferases From the UGT73C Subfamily Glycosylate Sapogenins, Forming a Spectrum of Mono- and Bisdesmosidic Saponins." *Plant Molecular Biology* 97: 37–55.
- Di Ferdinando, M., C. Brunetti, A. Fini, and M. Tattini. 2012. "Flavonoids as Antioxidants in Plants Under Abiotic Stresses." In *Abiotic Stress Responses in Plants*, edited by P. Ahmad and M. Prasad, New York, NY: Springer.
- Fraga, C. G., M. Galleano, S. V. Verstraeten, and P. I. Oteiza. 2010. "Basic Biochemical Mechanisms Behind the Health Benefits of Polyphenols." *Molecular Aspects of Medicine* 31: 435–445.
- Fujisawa, S., and Y. Kadoma. 2006. "Comparative Study of the Alkyl and Peroxy Radical Scavenging Activities of Polyphenols." *Chemosphere* 62: 71–79.
- Gabr, A. M. M., O. Sytar, H. Ghareeb, and M. Brestic. 2019. "Accumulation of Amino Acids and Flavonoids in Hairy Root Cultures of Common Buckwheat (*Fagopyrum esculentum*)." *Physiology and Molecular Biology of Plants* 25: 787–797.
- Gachon, C. M. M., M. Langlois-Meurinne, and P. Saindrenan. 2005. "Plant Secondary Metabolism Glycosyltransferases: The Emerging Functional Analysis." *Trends in Plant Science* 10: 542–549.
- Gechev, T., H. Willekens, M. Van Montagu, et al. 2003. "Different Responses of Tobacco Antioxidant Enzymes to Light and Chilling Stress." *Journal of Plant Physiology* 160: 509–515.
- Gharabli, H., V. Della Gala, and D. H. Welner. 2023. "The Function of UDP-Glycosyltransferases in Plants and Their Possible Use in Crop Protection." *Biotechnology Advances* 67: 108182.
- Griesser, M., F. Vitzthum, B. Fink, et al. 2008. "Multi-Substrate Flavonol O-Glucosyltransferases From Strawberry (*Fragaria* × *Ananassa*) Achene and Receptacle." *Journal of Experimental Botany* 59: 2611–2625.
- Hao, Y., X. Zong, P. Ren, Y. Qian, and A. Fu. 2021. "Basic Helix-Loop-Helix (bHLH) Transcription Factors Regulate a Wide Range of Functions in *Arabidopsis*." *International Journal of Molecular Sciences* 22: 7152.
- He, M., Y. He, K. Zhang, et al. 2022. "Comparison of Buckwheat Genomes Reveals the Genetic Basis of Metabolomic Divergence and Ecotype Differentiation." *New Phytologist* 235: 1927–1943.
- He, Q., D. Ma, W. Li, et al. 2023a. "High-Quality Genome Provides Insights into the Flavonoid Accumulation Among Different Tissues and Self-Incompatibility." *Journal of Integrative Plant Biology* 65: 1423–1441.
- He, Y., D. Ahmad, X. Zhang, et al. 2018. "Genome-Wide Analysis of Family-1 UDP Glycosyltransferases (UGT) and Identification of UGT Genes for FHB Resistance in Wheat (*Triticum aestivum* L.)." *BMC Plant Biology* 18: 67.
- He, Y., K. Zhang, and S. Li, et al. 2023b. "Multi-Omics Analysis Reveals the Molecular Mechanisms Underlying Virulence in Rhizoctonia and Jasmonic Acid-Mediated Resistance in Tartary Buckwheat (*Fagopyrum tataricum*)." *Plant Cell* 35, no. 8: 2773–2798.
- Huda, M. N., S. Lu, T. Jahan, et al. 2021. "Treasure From Garden: Bioactive Compounds of Buckwheat." *Food Chemistry* 335: 127653.
- Iqbal, H., C. Yaning, M. Waqas, S. T. Raza, M. Shareef, and Z. Ahmad. 2023. "Salinity and Exogenous H<sub>2</sub>O<sub>2</sub> Improve Gas Exchange, Osmoregulation, and Antioxidant Metabolism in Quinoa Under Drought Stress." *Physiologia Plantarum* 175: e14057.
- Irsyadi, M. B., S. K. Sari, E. Oktastuti, and I. A. Rineksane. 2024. "Rapid Genomic DNA Extraction for Soybean (*Glycine Max* L. Merr) Using Modified CTAB Protocol to Obtain High-Quality DNA." *Indian J Biochem Bio* 61: 97–104.
- Jiang, J., S. Ma, N. Ye, M. Jiang, J. Cao, and J. Zhang. 2017. "WRKY Transcription Factors in Plant Responses to Stresses." *Journal of Integrative Plant Biology* 59: 86–101.
- Jones, P., and T. Vogt. 2001. "Glycosyltransferases in Secondary Plant Metabolism: Tranquilizers and Stimulant Controllers." *Planta* 213: 164–174.
- Khan, R. A., and N. Abbas. 2023. "Role of Epigenetic and Post-Translational Modifications in Anthocyanin Biosynthesis: A Review." *Gene* 887: 147694.
- Kuzina, V., J. K. Nielsen, J. M. Augustin, A. M. Torp, S. Bak, and S. B. Andersen. 2011. "Barbarea Vulgaris Linkage Map and Quantitative Trait Loci for Saponins, Glucosinolates, Hairiness and Resistance to the Herbivore *Phyllotreta nemorum*." *Phytochemistry* 72: 188–198.
- Li, S., K. Zhang, M. Khurshid, Y. Fan, B. Xu, and M. Zhou. 2021. "First Report of *Rhizoctonia solani* AG-4 HGI Causing Stem Canker on *Fagopyrum tataricum*." *Plant Disease* 105: 505.
- Li, X., Z. Shi, J. Gao, X. Wang, and K. Guo. 2023. "Candihap: A Haplotype Analysis Toolkit for Natural Variation Study." *Molecular Breeding* 43: 21.
- Lim, C., K. Kang, Y. Shim, S. C. Yoo, and N. C. Paek. 2022. "Inactivating Transcription Factor OsWRKY5 Enhances Drought Tolerance Through Abscisic Acid Signaling Pathways." *Plant Physiology* 188: 1900–1916.
- Lim, E. K., D. A. Ashford, B. Hou, R. G. Jackson, and D. J. Bowles. 2004. "Arabidopsisglycosyltransferases as Biocatalysts in Fermentation for Regioselective Synthesis of Diverse Quercetin Glucosides." *Biotechnology and Bioengineering* 87: 623–631.
- Lippert, C., J. Listgarten, Y. Liu, C. M. Kadie, R. I. Davidson, and D. Heckerman. 2011. "FaST Linear Mixed Models for Genome-Wide Association Studies." *Nature Methods* 8: 833–835.
- Liu, J., A. Osbourn, and P. Ma. 2015. "MYB Transcription Factors as Regulators of Phenylpropanoid Metabolism in Plants." *Molecular Plant* 8: 689–708.
- Livak, K. J., and T. D. Schmittgen. 2001. "Analysis of Relative Gene Expression Data Using Real-Time Quantitative PCR and the 2<sup>-ΔΔCT</sup> Method." *Methods* 25: 402–408.
- Ma, T. L., W. J. Li, and Y. S. Hong, et al. 2022. "TMT Based Proteomic Profiling of *Sophora alopecuroides* Leaves Reveal Flavonoid Biosynthesis Processes in Response to Salt Stress." *Journal of Proteomics* 253: 104457.
- Mahajan, M., and S. K. Yadav. 2014. "Overexpression of a Tea Flavonone 3-Hydroxylase Gene Confers Tolerance to Salt Stress and *Alternaria solani* in Transgenic Tobacco." *Plant Molecular Biology* 85: 551–573.
- Mahmood, T., M. Abdullah, S. Ahmar, et al. 2020. "Incredible Role of Osmotic Adjustment in Grain Yield Sustainability Under Water Scarcity Conditions in Wheat (*Triticum aestivum* L.)." *Plants* 9: 1208.
- Marinova, K., L. Pourcel, B. Weder, et al. 2007. "Thearabidopsismate Transporter TT12 Acts as a Vacuolar Flavonoid/H<sup>+</sup>-Antiporter Active

- in Proanthocyanidin-Accumulating Cells of the Seed Coat." *Plant Cell* 19: 2023–2038.
- Martinez, V., T. C. Mestre, F. Rubio, et al. 2016. "Accumulation of Flavonols Over Hydroxycinnamic Acids Favors Oxidative Damage Protection Under Abiotic Stress." *Frontiers in Plant Science* 7: 838.
- Martín-García, B., F. Pasini, V. Verardo, A. M. Gómez-Caravaca, E. Marconi, and M. F. Caboni. 2019. "Distribution of Free and Bound Phenolic Compounds in Buckwheat Milling Fractions." *Foods* 8: 670.
- Meng, C., S. Zhang, Y. S. Deng, G. D. Wang, and F. Y. Kong. 2015. "Overexpression of a Tomato Flavanone 3-Hydroxylase-like Protein Gene Improves Chilling Tolerance in Tobacco." *Plant Physiology and Biochemistry* 96: 388–400.
- Mierziak, J., K. Kostyn, and A. Kulma. 2014. "Flavonoids as Important Molecules of Plant Interactions With the Environment." *Molecules* 19: 16240–16265.
- Morgan, J. T., G. R. Fink, and D. P. Bartel. 2019. "Excised Linear Introns Regulate Growth in Yeast." *Nature* 565: 606–611.
- Nakabayashi, R., K. Yonekura-Sakakibara, K. Urano, et al. 2014. "Enhancement of Oxidative and Drought Tolerance in *Arabidopsis* by Overaccumulation of Antioxidant Flavonoids." *Plant Journal* 77: 367–379.
- Ozturk, M., B. Turkyilmaz Unal, P. García-Caparrós, A. Khursheed, A. Gul, and M. Hasanuzzaman. 2021. "Osmoregulation and Its Actions During the Drought Stress in Plants." *Physiologia Plantarum* 172: 1321–1335.
- Ren, C., Z. Xi, B. Xian, et al. 2023. "Identification and Characterization of CtUGT3 as the Key Player of Astragalin Biosynthesis in *Carthamus tinctorius* L." *Journal of Agricultural and Food Chemistry* 71: 16221–16232.
- Riceevans, C. A., N. J. Miller, P. G. Bolwell, P. M. Bramley, and J. B. Pridham. 1995. "The Relative Antioxidant Activities of Plant-Derived Polyphenolic Flavonoids." *Free Radical Research* 22: 375–383.
- Slámová, K., J. Kapešová, and K. Valentová. 2018. "Sweet Flavonoids: Glycosidase-Catalyzed Modifications." *International Journal of Molecular Sciences* 19: 2126.
- Sleator, R. D. 2016. "JCVI-syn3.0-A Synthetic Genome Stripped Bare." *Bioengineered* 7: 53–56.
- Song, C., L. Gu, J. Liu, et al. 2015. "Functional Characterization and Substrate Promiscuity of UGT71 Glycosyltransferases From Strawberry (*Fragaria × Ananassa*)." *Plant and Cell Physiology* 56: 2478–2493.
- Tanenbaum, D. M., J. Goll, S. Murphy, et al. 2010. "The JCVI Standard Operating Procedure for Annotating Prokaryotic Metagenomic Shotgun Sequencing Data." *Standards in Genomic Sciences* 2: 229–237.
- Tanner, G. J., K. T. Francki, S. Abrahams, J. M. Watson, P. J. Larkin, and A. R. Ashton. 2003. "Proanthocyanidin Biosynthesis in Plants." *Journal of Biological Chemistry* 278: 31647–31656.
- Velasco, R., A. Zharkikh, J. Affourtit, et al. 2010. "The Genome of the Domesticated Apple (*Malus × Domestica* Borkh.)." *Nature Genetics* 42: 833–839.
- Verstraeten, S. V., C. G. Fraga, and P. I. Oteiza. 2015. "Interactions of Flavan-3-ols and Procyanidins With Membranes: Mechanisms and the Physiological Relevance." *Food and Function* 6: 32–41.
- Vogt, T., and P. Jones. 2000. "Glycosyltransferases in Plant Natural Product Synthesis: Characterization of a Supergene Family." *Trends in Plant Science* 5: 380–386.
- Wang, C., R. Jing, X. Mao, X. Chang, and A. Li. 2011. "TaABC1, a Member of the Activity of bcl Complex Protein Kinase Family From Common Wheat, Confers Enhanced Tolerance to Abiotic Stresses in *Arabidopsis*." *Journal of Experimental Botany* 62: 1299–1311.
- Wu, B., X. Liu, K. Xu, and B. Zhang. 2020. "Genome-Wide Characterization, Evolution and Expression Profiling of UDP-Glycosyltransferase Family in Pomelo (*Citrus grandis*) Fruit." *BMC Plant Biology* 20: 459.
- Wu, D., J. Luo, J. Chen, L. Zhang, K. J. Lim, and Z. Wang. 2019. "Selection Pressure Causes Differentiation of the SPL Gene Family in the Juglandaceae." *Molecular Genetics and Genomics* 294: 1037–1048.
- Xiao, X., Q. Lu, R. Liu, et al. 2019. "Genome-Wide Characterization of the UDP-Glycosyltransferase Gene Family in Upland Cotton." *3 Biotech* 9: 453.
- Xu, X., Y. Yan, W. Huang, et al. 2021. "Molecular Cloning and Biochemical Characterization of a New Coumarin Glycosyltransferase CtUGT1 From *Cistanche tubulosa*." *Fitoterapia* 153: 104995.
- Yang, F., L. Zhang, X. Zhang, et al. 2024. "Genome-Wide Investigation of UDP-Glycosyltransferase Family in Tartary Buckwheat (*Fagopyrum tataricum*)." *BMC Plant Biology* 24: 249.
- Yang, L., W. C. Li, and F. L. Fu, et al. 2022. "Characterization of Phenylalanine Ammonia-Lyase Genes Facilitating Flavonoid Biosynthesis From Two Species of Medicinal Plant." *PeerJ* 10: e13614.
- Yin, Q., X. Han, Z. Han, et al. 2020. "Genome-Wide Analyses Reveals a Glucosyltransferase Involved in Rutin and Emodin Glucoside Biosynthesis in Tartary Buckwheat." *Food Chemistry* 318: 126478.
- Youn, H. S., J. Y. Lee, S. I. Saitoh, et al. 2006. "Suppression of MyD88 and TRIF-Dependent Signaling Pathways of Toll-Like Receptor by (-)-Epigallocatechin-3-Gallate, a Polyphenol Component of Green Tea." *Biochemical Pharmacology* 72: 850–859.
- Yuan, Y., Y. J. Liu, and C. Wu, et al. 2012. "Water Deficit Affected Flavonoid Accumulation by Regulating Hormone Metabolism in Georgi Roots." *PLoS One* 7: e42946.
- Zamaratskaia, G., K. Gerhardt, M. Knicky, and K. Wendin. 2023. "Buckwheat: An Underutilized Crop With Attractive Sensory Qualities and Health Benefits." *Critical Reviews in Food Science and Nutrition* 64, no. 33: 12303–12318. <https://doi.org/10.1080/10408398.2023.2249112>.
- Zhang, F., X. Shi, J. Xu, W. Yuan, and Z. Li. 2024. "Tandem Gene Duplication Selected by Activation of Horizontally Transferred Gene in Bacteria." *Applied Microbiology and Biotechnology* 108: 340.
- Zhang, K., M. D. Logacheva, Y. Meng, et al. 2018. "Jasmonate-Responsive MYB Factors Spatially Repress Rutin Biosynthesis in *Fagopyrum tataricum*." *Journal of Experimental Botany* 69: 1955–1966.
- Zhang, K., Y. Sun, M. N. Li, and R. C. Long. 2021. "CrUGT87A1, a UDP-Sugar Glycosyltransferases (UGTs) Gene From *Carex rigescens*, Increases Salt Tolerance by Accumulating Flavonoids for Antioxidation in *Arabidopsis thaliana*." *Plant Physiology and Biochemistry* 159: 28–36.
- Zhang, K. X., M. He, Y. Fan, et al. 2021. "Resequencing of Global Tartary Buckwheat Accessions Reveals Multiple Domestication Events and Key Loci Associated With Agronomic Traits." *Genome Biology* 22: 23.
- Zhang, K. X., Y. Q. He, X. Lu, et al. 2023. "Comparative and Population Genomics of Buckwheat Species Reveal Key Determinants of Flavor and Fertility." *Molecular Plant* 16: 1427–1444.
- Zhang, L., X. Li, B. Ma, et al. 2017. "The Tartary Buckwheat Genome Provides Insights into Rutin Biosynthesis and Abiotic Stress Tolerance." *Molecular Plant* 10: 1224–1237.
- Zhang, M. H., S. Feng, S. Chen, Y. X. Zhou, C. Y. Gong, and W. Xue. 2023. "Synthesis, Antibacterial and Antifungal Activity of Myricetin Derivatives Containing Piperidine and Amide Fragments." *Pest Management Science* 79: 4795–4808.
- Zhao, H., Y. He, K. Zhang, et al. 2023. "Rewiring of the Seed Metabolome During Tartary Buckwheat Domestication." *Plant Biotechnology Journal* 21: 150–164.
- Zhao, J., and R. A. Dixon. 2010. "MATE Transporters Facilitate Vacuolar Uptake of Epicatechin 3'-O-Glucoside for Proanthocyanidin Biosynthesis in *Medicago truncatula* and *Arabidopsis*." *Plant Cell* 22: 991.
- Zhao, M., J. Jin, T. Gao, et al. 2019. "Glucosyltransferase CsUGT78A14 Regulates Flavonols Accumulation and Reactive Oxygen Species

Scavenging in Response to Cold Stress in *Camellia sinensis*.” *Frontiers in Plant Science* 10: 1675.

Zhao, Y., C. Q. Jiang, J. Y. Lu, Y. H. Sun, and Y. Y. Cui. 2023. “Research Progress of Proanthocyanidins and Anthocyanidins.” *Phytotherapy Research* 37: 2552–2577.

Zheng, Y. Z., G. Deng, Q. Liang, D. F. Chen, R. Guo, and R. C. Lai. 2017. “Antioxidant Activity of Quercetin and Its Glucosides From Propolis: A Theoretical Study.” *Scientific Reports* 7: 7543.

Zhou, J., C. L. Li, F. Gao, et al. 2016. “Characterization of Three Glucosyltransferase Genes in Tartary Buckwheat and Their Expression After Cold Stress.” *Journal of Agricultural and Food Chemistry* 64: 6930–6938.

### **Supporting Information**

Additional supporting information can be found online in the Supporting Information section.